

Nonstationary Intensity Statistics in Diffusive Waves

Ruitao Wu[✉] and Aristide Dogariu*

CREOL, The College of Optics and Photonics, University of Central Florida, Orlando, Florida 32816, USA

 (Received 4 February 2020; accepted 22 June 2020; published 21 July 2020)

It is a long-standing belief that, in the diffusion regime, the intensity statistics is always stationary and its probability distribution follows a negative exponential decay. Here, we demonstrate that, in fact, in reflection from strong disordered media, the intensity statistics changes through different stages of the diffusion. We present a statistical model that describes this nonstationary property and takes into account the evolving balance between recurrent scattering and near field coupling. The predictions are further verified by systematic experiments in the optical regime. This statistical nonstationary is akin to the nonequilibrium but steady-state diffusion of particulate systems.

DOI: [10.1103/PhysRevLett.125.043902](https://doi.org/10.1103/PhysRevLett.125.043902)

Intensity fluctuations are ubiquitous consequences of coherent waves encountering disordered media. The statistics of intensity fluctuations have been examined in various regimes of wave propagation, including the transition from ballistic to diffusion [1,2], the localization [3,4], and the superdiffusive regimes [5]. The common wisdom is that for waves in the diffusive regime, the intensity variation is a stationary random process that follows Rayleigh statistics.

However, when certain symmetries exist in low-dimensionality disordered systems, non-Rayleigh statistics occur contingent on the properties of incident waves [6–9]. Anomalous intensity statistics are also encountered in disordered media where deviations from the Rayleigh distribution are not due to properties of randomness [10–13]. Rather, they are caused by the varying contributions of stationary and propagating waves, which are specific to transition from closed to open systems [14].

Counterintuitively, the interaction with three-dimensional and highly disordered media does not necessarily guarantee the randomization of waves. It has been shown that when disorder increases, the waves can scatter recurrently and their trajectories can locally “loop” [15–17]. This mechanism reduces the diffusion coefficient and could also lead to the modifications of intensity statistics. Notably, there is also a competing process in random media; the near field coupling between scattering centers effectively destroys the “loops” created during diffusion [18]. This competition ultimately leads to a transition between different diffusion regimes [19], which suggests a statistical nonstationarity in the properties of waves during their propagation inside the diffusion regime.

In this Letter, we introduce a stochastic model that describes the diffusive waves as the superposition of two types of fields. Accounting for both recurrent scattering and near field coupling effects, the model predicts that the distribution of intensity fluctuations varies within the

volume of interaction. This nonstationary behavior is experimentally demonstrated in the optical regime.

When monochromatic waves propagate through non-dissipative, strongly scattering media, the steady-state field distribution can be regarded as the superposition of two fields with different stochastic properties. The first one corresponds to *traveling waves*, and, due to the inherent randomness of scattering, can be described as a Gaussian random process. In this component, the phase is uniformly distributed over $[-\pi, \pi]$ while the amplitude can be considered unity. As such, the distribution of local intensities follows a negative exponential function [20]. The second type of contributions correspond to waves that manifest phase correlations. Because of recurrent scattering events, waves can travel locally along counterpropagating trajectories, which leads to stochastic properties specific to *correlated waves*. In this case, the phases are no longer uniformly distributed, which is reminiscent of so-called partially developed speckle fields [21,22]. Without loss of generality, one can consider such waves as having constant amplitudes and the phases Gaussian distributed with zero mean and standard deviation σ_θ .

The above physical situation can be described by regarding the local field as the overlap of traveling $\vec{E}_t(\vec{r})$ and correlated $\vec{E}_c(\vec{r})$ waves:

$$\vec{E}(\vec{r}) = \frac{1}{\sqrt{N_1}} \sum_{m=1}^{N_1} e^{i(\theta_m + \vec{k}_m \cdot \vec{r})} + \varepsilon \frac{1}{\sqrt{N_2}} \sum_{n=1}^{N_2} e^{i(\theta_n + \vec{k}_n \cdot \vec{r})}. \quad (1)$$

These two components are the result of the superposition of N_1 and, respectively, N_2 plane waves. In Eq. (1), the corresponding phases and the wave vectors of these wave components are denoted by θ_m and θ_n and respectively, \vec{k}_m and \vec{k}_n . Note that these phases are independent random variables and θ_m is uniformly distributed over $[-\pi, \pi]$. The parameter ε measures the relative energetic contribution of

the two fields. This decomposition is somewhat similar to the field description in a disordered cavity that is only weakly coupled to the environment [14,23].

From Eq. (1) and the central limit theorem, one can now evaluate the joint probability density function (PDF) for the real and imaginary parts of phasor \vec{E} as detailed in the Supplemental Material [23]. The PDF of the intensity fluctuations $p_I(I)$, can also be obtained following a Jacobian transformation. It can be shown that

$$p_I(I) = \frac{1}{4\pi\sigma_{\mathbb{R}}\sigma_{\mathbb{I}}} \int_{-\pi}^{\pi} \exp\left[-\left(\frac{\sqrt{I}\cos\varphi - \mathbb{R}_0}{\sqrt{2}\sigma_{\mathbb{R}}}\right)^2 - \left(\frac{\sqrt{I}\sin\varphi}{\sqrt{2}\sigma_{\mathbb{I}}}\right)^2\right] d\varphi, \quad (2)$$

written in terms of $\sigma_{\mathbb{R}}^2 = \frac{1}{2} + (\varepsilon^2/2)[1 + \exp(-2\sigma_{\theta}^2)] - \varepsilon^2 \exp(-\sigma_{\theta}^2)$ and $\sigma_{\mathbb{I}}^2 = \frac{1}{2} + (\varepsilon^2/2)[1 - \exp(-2\sigma_{\theta}^2)]$, which are the standard deviations of the real and imaginary parts of the total field \vec{E} with the corresponding phase φ . Note that the interference among the correlated waves leads to a coherent background $\mathbb{R}_0 = \varepsilon\sqrt{N_2}\exp(-\sigma_{\theta}^2/2)$. Importantly, the values of $\sigma_{\mathbb{R}}$, $\sigma_{\mathbb{I}}$, and \mathbb{R}_0 depend only on three parameters: the standard deviation of the phase distribution σ_{θ} , the number of correlated waves N_2 , and the amplitude factor ε .

As follows from Eq. (2), the distribution of intensity fluctuations and, therefore, all its other measurable parameters depend on the statistical properties of the correlated components. Because of two competing mechanisms mentioned earlier, these properties may evolve during propagation and, consequently, the intensity statistics becomes a nonstationary process as depicted schematically in Fig. 1(a). When propagating through strongly disordered media, waves traveling over relatively small distances develop stronger phase correlations due to recurrent scattering. As the propagation progresses, the energy associated with this kind of waves leaks out through near-field coupling into different channels corresponding to propagating waves. This is the gradual transfer of energy from quasilocalized modes to propagating modes [19,24], which will therefore alter the distribution of intensity fluctuations.

To describe the evolution of the statistical nonstationarity of the intensity fluctuations, one needs to examine how the parameters σ_{θ} , N_2 , and ε depend on the propagation path length s . First of all, the PDF of the resultant field \vec{E} is an elliptical Gaussian distribution centered on the real axis of the complex plane, resembling a partially developed speckle [20]. Second, the standard deviation σ_{θ} of the phase distributions in the recurrent scattering loops is expected to be minimal and, meanwhile, ε is less than unity because the probability of recurrent scattering is rather small. Under these conditions, $\sigma_{\mathbb{R}} \approx \sigma_{\mathbb{I}}$, which means that the ellipticity of the PDF contour approaches unity. Therefore, when the statistical properties of the amplitude and the phase

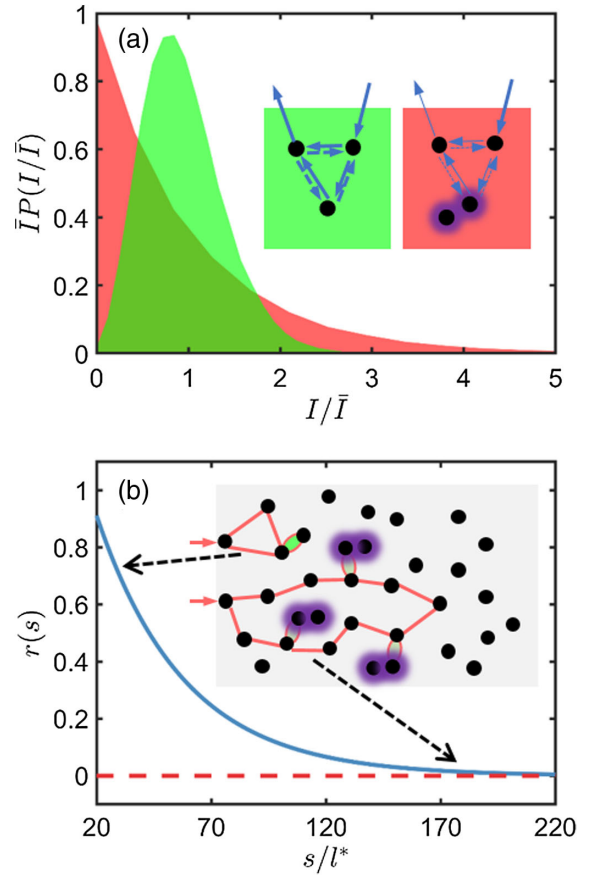


FIG. 1. Origin of PDF nonstationarity. (a) Strong recurrent scattering (green) at short paths leads to deviations from a negative exponential while near-field coupling (red) along longer paths tends to change it back. (b) The energy ratio $r(s)$ gauges the energetic contribution of correlated waves with respect to total energy. Because of the competition between creation of loops and energy leaking through near-field coupling, $r(s)$ depends on the trajectory length [blue curve, see Eq. (3)].

distributions do not vary significantly, the main consideration relates to the energetic contribution of correlated waves. This can be quantified by a dimensionless parameter $r(s) = \bar{T}_c(s)/\bar{I}(s) \approx [\varepsilon^2 N_2 \exp(-\sigma_{\theta}^2)]/[1 + \varepsilon^2 + \varepsilon^2 N_2 \exp(-\sigma_{\theta}^2)]$, which gauges the energetic contribution of the correlated waves with respect to the total energy. This parameter can be estimated using a mesoscopic description of wave transport in scattering medium that can be based on measurable properties as we show in the following.

In the mesoscopic theory of waves transport, the probability of recurrent scattering p_X is determined by the ratio between the trajectory volume and the volume explored by the waves [25], $p_X = \lambda^2/2l^{*2}$, which depends on the wavelength and the transport mean free path. During propagation, the energy corresponding to crossing channels of path length s leaks out due to near field coupling at a rate $\exp[-(3/2)n_0\bar{\sigma}_{\text{NF}}s]$, where n_0 is the number density of scatters and $\bar{\sigma}_{\text{NF}}$ is the near-field scattering cross

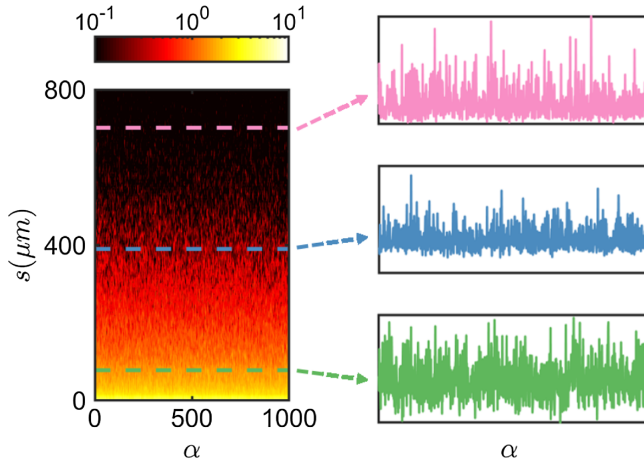


FIG. 2. Path-resolved intensity fluctuations for different realizations α of a semi-infinite inhomogeneous medium with 1.5 refractive index consisting of 50% volume fraction of TiO_2 particles with a diameter of $0.33 \mu\text{m}$. The intensity fluctuations corresponding to three different paths of length 80, 400, and $720 \mu\text{m}$ are shown on the right panels.

section [26]. Therefore, the energy ratio $r(s)$ varies along paths of increasing path length as

$$r(s) = \frac{\lambda^2}{2l^{*2}} \exp\left(-\frac{3n_0\overline{\sigma}_{\text{NF}}}{2}s\right). \quad (3)$$

An example of this evolution is also illustrated in Fig. 1(b) for waves with 1310 nm wavelength interacting with a strongly scattering medium consisting of 330 nm spheres with refractive index of 2.3 packed randomly at 50% volume fraction. The transport mean free path l^* and the near field scattering cross section $\overline{\sigma}_{\text{NF}}$ are calculated following the approaches in Refs. [18] and [26], respectively.

As seen in Fig. 1, the energetic contribution of the correlated waves diminishes gradually because of the competing mechanism of loops creation due to randomness and the loops fading due to energy leaking through near field interactions. Thus, the statistics of intensity fluctuations changes when the interaction path length varies. The energetic parameter defined in Eq. (3) measures the contribution of correlated waves and, therefore, it determines the various features of the intensity statistics. In other words, $r(s)$ determines the deviation of intensity fluctuations PDF from a negative exponential.

To demonstrate experimentally the predictions of this statistical model, we performed path-length-resolved measurements of light reflected from strongly disorder media. Using the optical path-length spectroscopy [27], path-length-resolved intensity patterns were recorded for different realizations of randomness [23]. The interferometric measurement uses a partially coherent source with a central wavelength of 1310 nm and the temporal resolution of about 100 fs. Random media with different volume fractions (from 2.5% to 50%) were prepared using $0.33 \mu\text{m}$ -in-diameter

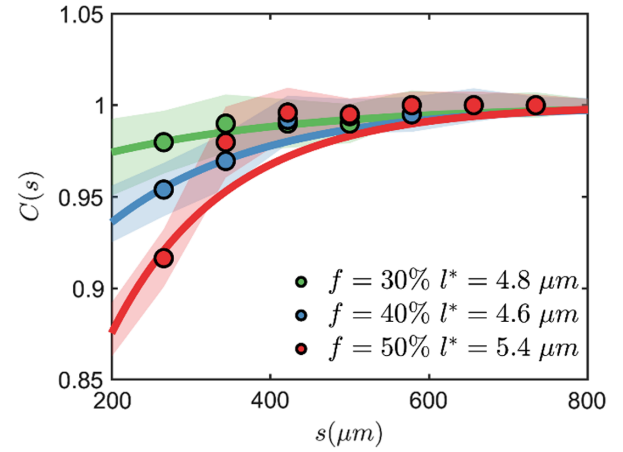


FIG. 3. Path-length-resolved normalized variance (contrast) of intensity fluctuations in strong scattering media displaying sub-diffusive behavior of propagation. The solid lines denote the evaluations based on mesoscopic wave transport theory in Eq. (3). The dots are the corresponding experimental results for media with different volume fractions and transport mean free paths as indicated. The shaded areas represent the standard deviation of five different datasets, each including 200 measurements.

TiO_2 particles (refractive index 2.3) embedded in a polymer matrix with refractive index of 1.5. For each sample, we collected an ensemble of 1000 measurements corresponding to different realizations of the random medium.

Typical results are illustrated in Fig. 2 for the specific case of a sample with 50% volume fraction of scattering centers. As evident in the right panels, for longer and longer paths through the medium, the intensity fluctuations change their statistical properties. These changes can be quantified by the normalized variance of intensity fluctuations (speckle contrast) that varies with the path length as shown in Fig. 3 (dots). To the best of our knowledge, this is the first time that the second order statistics of the intensity fluctuations are analyzed as a function of wave path length. In the experiment, the effects of polarization and detection noise have been carefully removed.

The scattering strength of different random media can be gauged by an averaged transport mean free path l^* . Note that the absorption coefficient of TiO_2 in this wavelength is negligible. For each sample, l^* is evaluated from measurements using a bistatic reflection technique capable of providing information independent of particular surface conditions [28]. The corresponding values are indicated in the legend of Fig. 3. Note that, starting from pathlengths longer than $s = 200 \mu\text{m}$, for the three selected samples with high volume fraction, light has already traveled more than $30 l^*$ through the medium, which ensures that the measurements correspond to the diffusion regime [29].

As we mentioned before, under the assumption of small σ_θ , the PDF deviation from a negative exponential can be characterized by $r(s)$, as the distribution of intensity fluctuations converges towards a modified Rician distribution [20].

In this limit, the correlated waves generate a coherent, but not necessarily uniform background that reduces the normalized variance according to $C(s) = \sqrt{1 - r(s)^2}$, where $r(s)$ is evaluated from Eq. (3). This is illustrated in Fig. 3, where, for all the samples, the experimental results are very well described by the model based on the mesoscopic theory of waves transport. The small deviation in the case of 50% medium indicates that, at such high packing fraction, the simple model in terms of isolated leaking events in Eq. (3) may not be sufficient anymore; a more specific description is necessary to describe the rapid transition to the uncorrelated regime.

Let us now discuss the significance of these results. First of all, one could argue that, no matter how the multiple scattering process evolves inside a scattering medium, a portion of the initial coherent field is still present, which could represent the ‘‘correlated contribution.’’ This would also lead to a monotonic increase of the normalized variance with increasing path lengths because the ballistic component degrades as waves penetrate deeper inside the medium. Such a gradual transition from ballistic to diffusive regimes has been studied extensively [2]. Naively, one could consider that the ballistic component, i.e., the coherent background, decays as $\exp[-(s/2 + z_0)/l^*]$, where z_0 is a boundary correction as suggested in Ref. [30] and l^* is calculated following Ref. [18]. Based on this argument, an estimation of the normalized variance $C = 0.96$ for all samples is indicated by the pink dotted line in Fig. 4. This particular value was chosen arbitrarily but it is representative for the so-called fully developed speckles. One would expect that this value is reached for smaller and smaller path lengths when increasing the scatterer density and correspondingly reducing the scattering mean free path.

As clearly indicated by the solid dots in Fig. 4, we find experimentally that this value of $C = 0.96$ is reached only for significantly deeper penetrations into random media with volume fractions ranging from 2.5% to 50%. The error bars represent the standard deviations corresponding to five different datasets each based on 200 independent measurements. It is also evident that for low concentrations, the simple ballistic attenuation argument makes a reasonable description of the experimental data. In this regime, the cutoff path length reduces with increasing the volume fraction because the waves scatter progressively more for the same over all path lengths.

However, with increasing volume fraction f , this simple explanation becomes insufficient. The pink dotted line deviates significantly from the experimental values. For strongly scattering media with $f > 30\%$, one expects the emergence of the competing mechanisms of recurrent scattering and near-field energy leaking [19]. These contributions are not accounted in the conventional treatment of the statistical properties of scattered waves. We note that, importantly, this situation happens not in the transition from ballistic to diffusion, but rather deep inside the diffusion

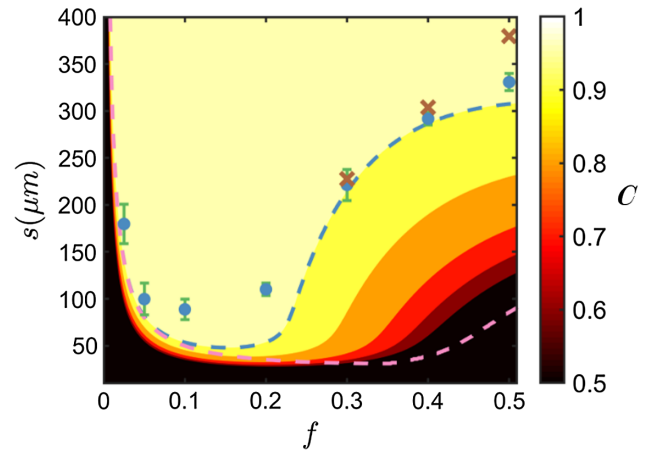


FIG. 4. Contour plot of the normalized variance (contrast) of intensity fluctuations for waves propagating along different path lengths through random media with varying volume fractions. The pink dotted line indicates the normalized variance of $C = 0.96$ calculated based on a ballistic attenuation model (see text). The blue dotted line indicates the theoretical prediction for the same value $C = 0.96$ using the model based on Eq. (3). The blue solid dots denote the experimental path lengths for which the same value of normalized variance is attained. The error bars designate the standard deviations from five different datasets, while each includes 200 measurements. The brown crosses indicate the path lengths for which the phase transitions are observed in the diffusion of light (see text).

regime. Using the mesoscopic model in Eq. (3), one can evaluate the intensity normalized variance C as a function of both path-length and scattering strength as a contour plot in Fig. 4. We also indicated, with the blue dotted line, the value of $C = 0.96$, which, in this case, corresponds to path lengths that agree quite well with the experimental results.

We would like to emphasize that, in Fig. 4, the region above the pink dotted line can be interpreted as the conventional diffusive regime where complete randomness is assumed and, consequently, the statistics is expected to obey the Rayleigh law of Gaussian statistics. However, the experiments indicate that this happens practically only above the blue dotted line. In the region between these two lines, the phase of the random waves is not uniformly distributed primarily because of the recurrent scattering as explained here. As the wave penetrates deeper into the medium, the probability distribution of the intensity fluctuations starts to conform to a negative exponential function.

The path-length threshold for which a complete phase randomization occurs is determined by the average penetration depth at which the balance is reached between the on-shell and off-shell wave manifestations indicating a new phase in the waves diffusion [25]. The path lengths at which this phase transition occurs are indicated by the brown symbols in Fig. 4. The difference is due to the arbitrary normalized variance value 0.96 chosen for this comparison. Above this threshold, a steady state establishes, which is similar to the thermodynamic equilibrium reached at longer

times by particles diffusing under the influence of random but finite-strength potentials.

We would like to add a final comment regarding the evolution of the intensity variance. By analogy with thermal diffusion of particulates, the path-length region between the dotted lines in Fig. 4 can be regarded as the transitional domain between a subdiffusional regime and the final steady-state diffusion of particles exposed to random potentials [31–35]. The extent of this transition depends not only on the average strength of the potential but also on its spatial correlation [36]. Thus, the statistical nonstationarity we identified in the intensity fluctuations gauges how the steady-state equilibrium is reached for different random media. This process is rather fast at low f but it evolves slower at higher concentrations when the scattering potentials are increasingly more correlated. In our case, the diffusion is constrained by the effective random potential created by strong local interferences leading to weak correlations between the partial waves that contribute to the detected intensity. The waiting times at these confining locations is determined by the strength of the evanescent coupling between the structural elements of the random medium.

Conclusions.—The average distribution of intensity is rather well understood for different regimes of wave propagation [37,38]. Here we demonstrate that in strongly scattering media, the competition between the mechanisms of recurrent scattering and energy leaking through near field coupling determines an evident nonstationarity in the intensity statistics. Surprisingly, this happens in the diffusion regime where an assumption of complete wave randomization had been widely used. The phenomenon resembles the coupling between waves with different phase properties encountered with disorder cavities with tunable properties [39,40].

As intensity fluctuations are rather easily accessible, our results provide practical means to describe how the process of wave propagation in random media evolves from having a specific subdiffusive behavior to a long-time diffusion regime as required, at large scales, by the ultimate thermal equilibrium.

We have shown here that the normalized variance of intensity fluctuations is a nonstationary property that depends on intrinsic characteristics of the scattering medium. Aside from the direct relevance to characterizing and engineering materials with controlled properties, our results also suggest a convenient optical testbed for studying the anomalous transport phenomena in nonequilibrium conditions pertinent to most natural processes [41–44].

This work was partially supported by the Office of Naval Research (N00014-18-1-2262).

*Corresponding author.

adogariu@creol.ucf.edu

[1] R. Elaloufi, R. Carminati, and J.-J. Greffet, *J. Opt. Soc. Am. A* **21**, 1430 (2004).

- [2] A. A. Chabanov and A. Z. Genack, *Phys. Rev. E* **56**, R1338 (1997).
- [3] M. Stoytchev and A. Z. Genack, *Opt. Lett.* **24**, 262 (1999).
- [4] A. A. Chabanov, M. Stoytchev, and A. Z. Genack, *Nature (London)* **404**, 850 (2000).
- [5] P. Barthelemy, J. Bertolotti, and D. S. Wiersma, *Nature (London)* **453**, 495 (2008).
- [6] H. E. Kondakci, A. Szameit, A. F. Abouraddy, D. N. Christodoulides, and B. E. A. Saleh, *Optica* **3**, 477 (2016).
- [7] H. E. Kondakci, A. F. Abouraddy, and B. E. A. Saleh, *Nat. Phys.* **11**, 930 (2015).
- [8] H. E. Kondakci, A. F. Abouraddy, and B. E. A. Saleh, *Optica* **2**, 201 (2015).
- [9] H. E. Kondakci, A. Szameit, A. F. Abouraddy, D. N. Christodoulides, and B. E. A. Saleh, *APL Photonics* **2**, 071301 (2017).
- [10] E. Kogan, M. Kaveh, R. Baumgartner, and R. Berkovits, *Phys. Rev. B* **48**, 9404 (1993).
- [11] N. Garcia and A. Z. Genack, *Phys. Rev. Lett.* **63**, 1678 (1989).
- [12] N. Shnerb and M. Kaveh, *Phys. Rev. B* **43**, 1279 (1991).
- [13] A. Apostol and A. Dogariu, *Phys. Rev. E* **72**, 025602(R) (2005).
- [14] R. Pnini and B. Shapiro, *Phys. Rev. E* **54**, R1032 (1996).
- [15] D. S. Wiersma, M. P. van Albada, B. A. van Tiggelen, and A. Lagendijk, *Phys. Rev. Lett.* **74**, 4193 (1995).
- [16] A. Aubry, L. A. Cobus, S. E. Skipetrov, B. A. van Tiggelen, A. Derode, and J. H. Page, *Phys. Rev. Lett.* **112**, 043903 (2014).
- [17] M. Störzer, P. Gross, C. M. Aegerter, and G. Maret, *Phys. Rev. Lett.* **96**, 063904 (2006).
- [18] R. R. Naraghi, S. Sukhov, J. J. Sáenz, and A. Dogariu, *Phys. Rev. Lett.* **115**, 203903 (2015).
- [19] R. R. Naraghi and A. Dogariu, *Phys. Rev. Lett.* **117**, 263901 (2016).
- [20] J. W. Goodman, *Speckle Phenomena in Optics: Theory and Applications* (Roberts and Company Publishers, Englewood, 2007).
- [21] E. Jakeman, *Opt. Eng. (Bellingham, Wash.)* **23**, 453 (1984).
- [22] J. Ohtsubo and T. Asakura, *Optik (Stuttgart)* **45**, 65 (1976).
- [23] See Supplemental Material at <http://link.aps.org/supplemental/10.1103/PhysRevLett.125.043902> for the connection of the proposal description to the field statistics in an open and closed random system (S1), and detailed information regarding the optical path-length resolved fluctuations measurement (S3).
- [24] N. Cherroret, T. Karpiuk, B. Grémaud, and C. Miniatura, *Phys. Rev. A* **92**, 063614 (2015).
- [25] E. Akkermans and G. Montambaux, *Mesoscopic Physics of Electrons and Photons* (Cambridge University Press, New York, 2007).
- [26] A. Y. Bekshaev, K. Y. Bliokh, and F. Nori, *Opt. Express* **21**, 7082 (2013).
- [27] G. Popescu and A. Dogariu, *Opt. Lett.* **24**, 442 (1999).
- [28] K. M. Douglass and A. Dogariu, *Opt. Lett.* **34**, 3379 (2009).
- [29] K. M. Yoo, F. Liu, and R. R. Alfano, *Phys. Rev. Lett.* **64**, 2647 (1990).

- [30] D. Contini, F. Martelli, and G. Zaccanti, *Appl. Opt.* **36**, 4587 (1997).
- [31] R. D. L. Hanes, M. Schmiedeberg, and S. U. Egelhaaf, *Phys. Rev. E* **88**, 062133 (2013).
- [32] P. Tierno, F. Sagués, T. H. Johansen, and I. M. Sokolov, *Phys. Rev. Lett.* **109**, 070601 (2012).
- [33] M. A. Despósito, *Phys. Rev. E* **84**, 061114 (2011).
- [34] R. Zwanzig, *Proc. Natl. Acad. Sci. U.S.A.* **85**, 2029 (1988).
- [35] L. F. Cugliandolo, *J. Phys. A* **44**, 483001 (2011).
- [36] M. Schmiedeberg, J. Roth, and H. Stark, *Eur. Phys. J. E* **24**, 367 (2007).
- [37] P. Sheng, *Introduction to Wave Scattering, Localization and Mesoscopic Phenomena* (Springer Science & Business Media, New York, 2006), Vol. 88.
- [38] S. E. Skipetrov and I. M. Sokolov, *Phys. Rev. Lett.* **123**, 233903 (2019).
- [39] J.-B. Gros, P. del Hougne, and G. Lerosey, *Phys. Rev. A* **101**, 061801 (2020).
- [40] D. V. Savin, M. Richter, U. Kuhl, O. Legrand, and F. Mortessagne, *Phys. Rev. E* **96**, 032221 (2017).
- [41] D. Villamaina, *Transport Properties in Non-Equilibrium and Anomalous Systems* (Springer Science & Business Media, New York, 2013).
- [42] U. Ray, G. K.-L. Chan, and D. T. Limmer, *Phys. Rev. Lett.* **120**, 210602 (2018).
- [43] X.-J. Zhang, H. Qian, and M. Qian, *Phys. Rep.* **510**, 1 (2012).
- [44] U. Seifert and T. Speck, *Europhys. Lett.* **89**, 10007 (2010).